Nanotechnology

PAPER • OPEN ACCESS

Synthesis of folic acid functionalized gold nanoclusters for targeting folate receptor-positive cells

To cite this article: Zhimin Liu *et al* 2019 *Nanotechnology* **30** 505102

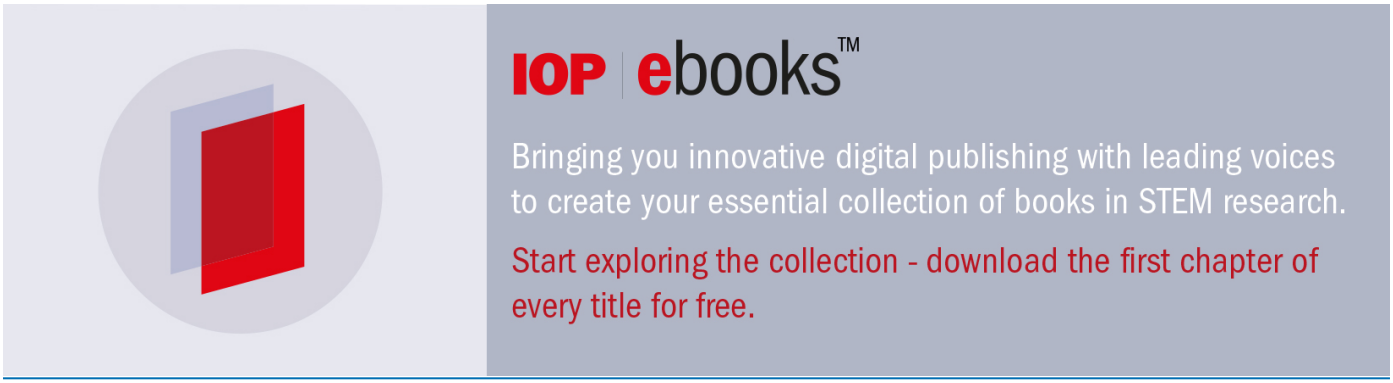

OPEN ACCESS
IOP Publishing
Nanotechnology

Nanotechnology **30** (2019) 505102 (7pp)
https://doi.org/10.1088/1361-6528/ab437c

Synthesis of folic acid functionalized gold nanoclusters for targeting folate receptor-positive cells

Zhimin Liu[1], Lyudmila Turyanska[2,3,8], Francesco Zamberlan[1], Salvatore Pacifico[4], Tracey D Bradshaw[5], Fabrizio Moro[2,6], Michael W Fay[7], Huw E L Williams[1] and Neil R Thomas[1,8]

[1] Centre for Biomolecular Sciences, School of Chemistry, The University of Nottingham, University Park, Nottingham NG72D, United Kingdom
[2] School of Physics and Astronomy, The University of Nottingham, University Park, Nottingham NG72D, United Kingdom
[3] School of Chemistry, University of Lincoln, Lincoln LN6 7DL, United Kingdom
[4] Department of Chemical and Pharmaceutical Sciences, University of Ferrara, Via Fossato di Mortara 17, I-44121, Ferrara, Italy
[5] School of Pharmacy, The University of Nottingham, University Park, Nottingham NG72D, United Kingdom
[6] Department of Materials Science, University of Milano-Bicocca, via R. Cozzi 55, 20125, Milan, Italy
[7] Nanoscale and Microscale Research Centre, The University of Nottingham, University Park, Nottingham NG72D, United Kingdom

E-mail: Lyudmila.Turyanska@nottingham.ac.uk and Neil.Thomas@nottingham.ac.uk

Received 28 January 2019, revised 23 August 2019
Accepted for publication 11 September 2019
Published 3 October 2019

Abstract

We report on the synthesis of water-soluble gold nanoclusters capped with polyethylene glycol (PEG)-based ligands and further functionalized with folic acid for specific cellular uptake. The dihydrolipoic acid-PEG-based ligands terminated with –OMe, $–NH_2$ and –COOH functional groups are produced and used for surface passivation of Au nanoclusters (NCs) with diameters <2 nm. The produced sub 2 nm Au NCs possess long-shelf life and are stable in physiologically relevant environments (temperature and pH), are paramagnetic and biocompatible. The paramagnetism of Au NCs in solution is also reported. The functional groups on the capping ligands are used for direct conjugation of targeting molecules onto Au NCs without the need for post synthesis modification. Folic acid (FA) is attached *via* an amide group and effectively target cells expressing the folate receptor. The combination of targeting ability, biocompatibility and paramagnetism in FA-functionalized Au NCs is of relevance for their exploitation in nanomedicine for targeted imaging.

Supplementary material for this article is available online

Keywords: gold nanocluster, paramagnetic, folic acid, targeting folate receptor

(Some figures may appear in colour only in the online journal)

[8] Author to whom any correspondence should be addressed.

Over the past decade, applications for colloidal nanoparticles have emerged in bioimaging and nanomedicine, with research efforts focusing on their formation and improving the stability in aqueous solutions [1–3]. The optical and electronic properties of Au nanoparticles change when their diameter is

smaller than 2 nm, and they are referred to as nanoclusters (NCs). Recent progress in the field has led to the emergence of ultra-small metal nanoclusters, including gold nanoclusters (Au NCs) [4], which exhibit discrete, molecule-like energy levels, tuneable optical properties and are biocompatible [5, 6], making them promising candidates for a range of applications, from bioimaging [7] to biosensing [8] and catalysis [9].

A pathway for the generation of Au NCs in aqueous solution was developed by Susumu *et al* [10] and follows the Brust-Schiffrin method using lipoic acid (LA) esterified to polyethylene glycol (PEG) as capping ligands. PEG- and LA-PEG-molecules have been successfully used for water solubilization and biological compatibility in a range of nanomaterials [11], including semiconductor quantum dots [12, 13] and metal nanoparticles [13, 14]. The incorporation of amino- or carboxyl-termini onto the PEG chain allows further modification including the attachment of targeting ligands, such as peptides, small proteins, and antibodies [11, 13].

In recent years, Au NCs have been functionalized for targeted therapy and bioimaging [15, 16], with particular interest in functionalization with folic acid (FA) for targeting to folate receptors, which are overexpressed in breast, colon, rectal and prostate cancer cells [17]. The targeting ability of FA has been previously demonstrated for iron oxide nanoparticles (NPs) [18], upconverting rare earth nanoparticles [19] and Au NPs [15, 20, 21]. Functionalization of Au NCs with targeting molecules remains challenging, but has been achieved for nanoparticles with gold core diameters of 2–6 nm using polymeric linkers [15], via conjugation to bovine serum albumin-stabilized particles [16]. Direct attachment of FA was demonstrated only for larger particles [22]. Indeed, direct attachment of FA onto NCs would be beneficial to avoid significant increases in the overall size and hence properties of the Au NCs, however, to date, this has not been demonstrated.

Here we describe the synthesis, chemical and physical characterization, stability and cell targeting abilities of colloidal, water soluble Au NCs with core diameters from 1.7 to 2.2 nm. The effects of ligand length, terminal functional group and the ratio of reactants on morphological, optical and magnetic properties of Au NCs are also reported. For direct attachment of FA, LA-PEG-based capping ligands terminated with $-NH_2$ were used. The stability of FA-functionalized NCs has been explored under physiologically relevant conditions and the cytotoxicity has been assessed *in vitro*. The targeting ability of FA-Au NCs has been confirmed with FA receptor expressing cancer cells.

We have synthesized LA-PEG_{200} and LA-PEG_{400} capping ligands with amine (LNH_2), methoxy (LOMe) and carboxylic acid (LCOOH) terminal functional groups (figure 1(a)) to produce aqueous colloidal Au NC solutions. Briefly, chloroauric acid was used as a source of gold, mixed with ligands under alkaline conditions (pH $\sim$ 11) in deionized water and reduced using $NaBH_4$. We have examined the effect of different molar ratios of Au:Ligand (from 1:0.2 to 1:10) and Au:$NaBH_4$ on the size and colloidal stability of

Figure 1. (a) Cartoon of an Au nanocluster capped with DHLA-PEG ligands terminated with different functional groups. (b) TEM and HR TEM images of Au NC capped with LA-PEG200-based ligands with NH_2 functional ending group.

produced AuNCs. We found that with increasing the Au:ligand ratio from 1:1 to 1:5, the average diameter decreases from 1.9 ± 0.3 nm to 1.7 ± 0.3 nm (supplementary information S1 is available online at stacks.iop.org/NANO/30/505102/mmedia). The ratio of Au:Ligand of 1:3, Au:reducing agent of 1:2 and aging time of 20 h produced AuNCs with sub 2 nm sizes and their colloidal solutions demonstrated long-shelf life and have narrow size distribution. Purification of the NCs was achieved by centrifugation and filtration (molecular weight cut-off 10 kDa), producing a concentrated brown solution. The stability of these AuNCs was confirmed against physiologically relevant conditions of pH = 3.0–10.0 and temperatures $T = 40\,^{\circ}C$ and $50\,^{\circ}C$. Exposure of the AuNC solution to different pH and/or T, did not induce any noticeable changes to their optical and morphological properties, as assessed by UV–vis and TEM, respectively (see supplementary information S2).

HR TEM analysis revealed that Au NCs capped with LNH_2 with an Au:ligand ratio of 1:3 possessed an average diameter $d_{AuNP} = 1.8 \pm 0.4$ nm; the crystalline structure of PEG-Au NCs can be clearly seen in figure 1(b), with an interplane distance of 2.34 Å, which corresponds to the gold face centred cubic (FCC) structure phase of (111) [23]. Dark field TEM studies revealed the presence of a thick carbon-based amorphous layer surrounding the nanocrystal: the non-uniform depth of the amorphous layer and the interparticle distance of $\geqslant$2 nm suggests that the LA-PEG_{200} ligands are not closely packed and have significant flexibility to re-orientate (see supplementary information, S1). Their position is random and the density of the ligand shell is such that ligand

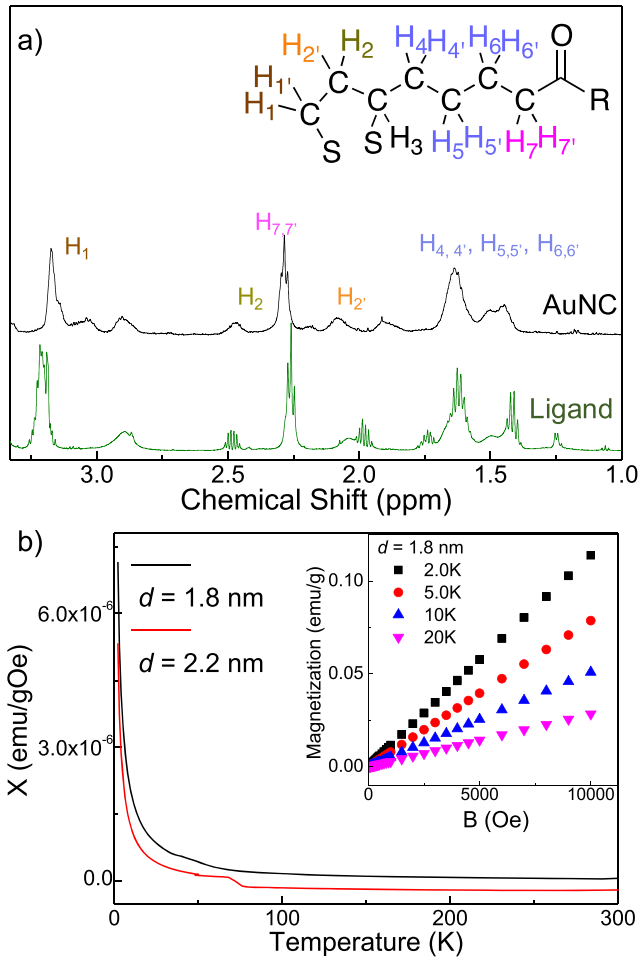

Figure 2. (a) Representative ^{1}H-NMR spectra of the ligand alone (black) and attached to the surface of a Au NC (green). Inset shows chemical structure of the ligand with assigned protons. (b) SQUID measurements of magnetic susceptibility and magnetization (inset) for Au NCs with diameters of 1.8 and 2.2 nm.

interlocking between neighbouring nanocrystals is possible [24]. We note that the NCs can be prepared with PEG-based ligands of different length, from PEG_{200} to PEG_{2000} (approximate length of stretched molecules is 3 nm and 10 nm, respectively). The average Au core diameter of the NCs formed is not affected by either the length of the polymer chain, nor by the type of the terminal group (–NH_2, –COOH, –OMe) (see supplementary information, S1).

The ^{1}H-NMR reported in figure 2(a) shows the comparison of the relevant chemical shifts between the synthesized ligand and the ligand attached to the surface. Broadening of the signal is observed, as expected due to faster relaxation rates resulting from slower tumbling of the NP, but also could result from the presence of paramagnetic NCs. Indeed, theoretical work predicts that Au NPs with sizes <2 nm are expected to have paramagnetic properties and these were confirmed for the NC films [25]. We experimentally observe magnetism in the Au NC films by the measurement of magnetization and in the Au NC solutions by shortening of the proton relaxation time, T_1.

Our magnetic studies using a superconducting quantum interference device (SQUID) on the Au NPs with sizes 1.8 and 2.2 nm show that at low temperatures ($T < 50$ K) the nanoparticles are paramagnetic and the 1.8 nm NCs possess magnetic susceptibility which gradually decreases from 2 K (7.16×10^{-6} emu/gOe versus 5.33×10^{-6} emu/gOe) to 50 K (0.44×10^{-6} emu/gOe versus 0.15×10^{-6} emu/gOe) (figure 2(b) and supplementary information, S1). For Au NCs with diameter of 1.8 nm the paramagnetic properties are observable up to room temperature.

In our NMR studies, we observed significant shortening of the longitudinal relaxation time, T_1, for protons in the capping ligands of Au NCs compared to that for protons in the ligand only. We note that the biggest difference is observed for the protons in the immediate proximity of the NC core (T_1 decreases from 1.61 to 0.64 s), as was shown previously for paramagnetic quantum dots [26] (see also supplementary information, S1). The observation of magnetism in AuNCs is of potential interest for their application in magnetic resonance imaging. Combined magnetism and targeting of the NCs could be used for development of novel diagnostic and therapeutic approaches. This potential development requires further detailed investigation.

FA was attached to LA-PEG ligands by a direct coupling reaction with LA-PEG-NH_2 in the presence of the standard peptide coupling reagents *N*-(3-dimethylaminopropyl)-*N*′-ethylcarbodiimide (EDC) and *N*-hydroxysuccinimide (NHS) (figure 3(a) and supplementary information, S2). The structure of the ligand shown in the figure 3(a) illustrates one molecule of lipoic acid (LA) covalently attached to one molecule of PEG and the amine at the terminating end of the LA-PEG coupled with one molecule of folic acid. The EDC and NHS were used to activate the available carboxyl groups of FA for coupling to the primary amine of LA-PEG-NH_2. We note that this method is non-regioselective and the reaction occurs with either of the FA carboxylates. Successful attachment of FA was confirmed by mass ESI micro TOF spectroscopy, where the negative ion peak for the species is seen at 802.2991 m/z (see supplementary information S3).

The LA-PEG-FA produced was used to functionalize Au NCs following the same procedure employed for LA-PEG-capped Au NCs. The FA-ligands provide efficient capping of the Au NCs and do not dramatically affect the morphology nor the colloidal stability of the nanoclusters. The dynamic light scattering (DLS) measurements show that the hydrodynamic size of the NCs is increased following functionalization with the FA, from 4.8 ± 1.3 nm to 6.5 ± 1.6 nm (figure 3(b)). The successful attachment is also supported by UV/Vis studies (figure 3(c)), where an absorption band at ~370 nm characteristic for FA [27] is observed for FA-Au NC, but not for Au NCs only. We note, that the synthesis of the targeted ligand is performed with FA the limiting reagent with respect to LA-PEG and any excess of reagents and starting materials is removed during purification steps, prior to using LA-PEG-FA ligand for the synthesis of the Au NCs.

Our HR TEM studies revealed the presence of Au NCs with an average diameter of $d_{AuNP} = 1.6 \pm 0.3$ nm (figure 3(d)). An increase in interparticle spacing (>4 nm)

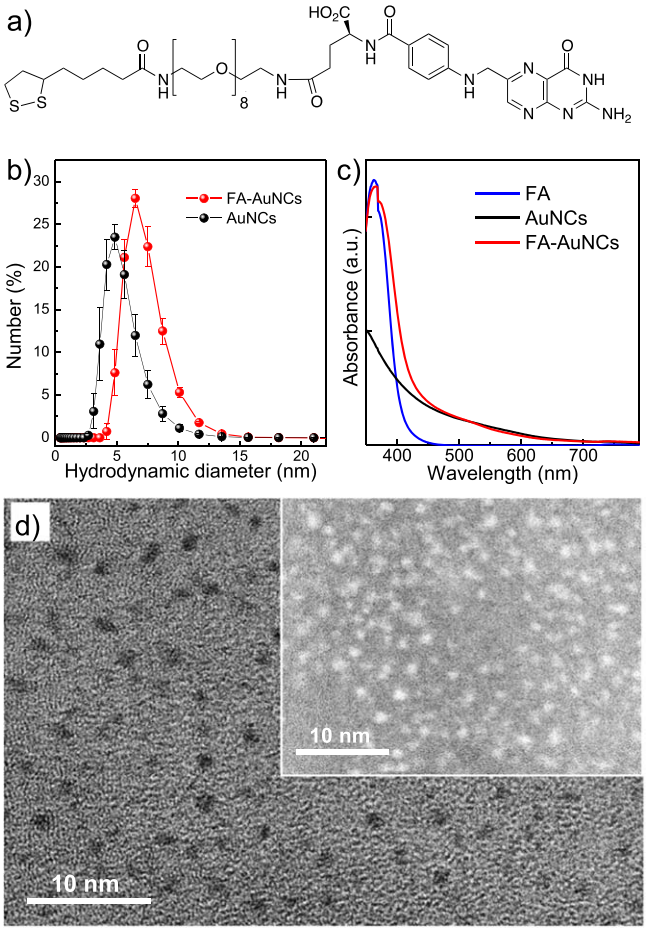

Figure 3. (a) Chemical structure of folic acid conjugated ligand. (b) Hydrodynamic diameter of the Au NCs and FA-Au NCs measured by DLS. (c) UV–vis spectra of Au NC (black), Au NC-FA (red) and FA (blue). (d) Representative TEM and (inset) dark field images of FA conjugated Au NCs.

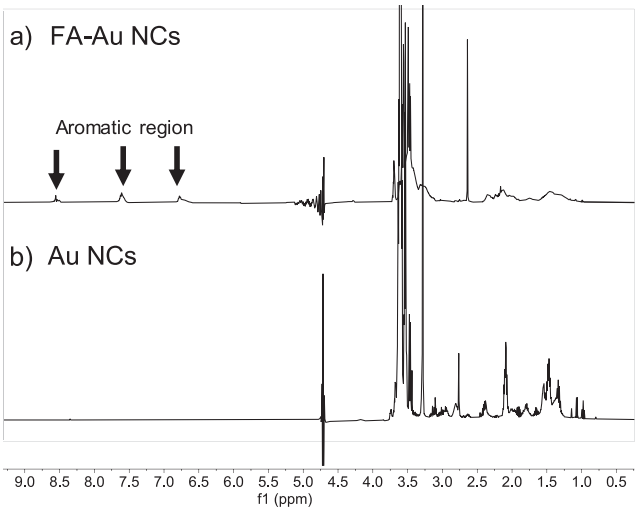

Figure 4. ^{1}H-NMR spectra of (a) FA-Au NCs and (b) Au NCs, evidencing peaks of aromatic protons on the folic acid moiety indicated by arrows. Observed artifact at ~4.7 ppm is due to excitation sculpting for water peak suppression.

compared to non functionalized NCs, is also observed in the bright- and dark-field TEM images (Inset in figure 3(d) and supplementary information S1, figure S2), indicating the presence of longer ligands consistent with the presence of FA on the NCs. This interpretation supports our observation of larger hydrodynamic diameter for FA-Au NCs compared to non-targeted Au NCs in our DLS measurements.

The ^{1}H-NMR spectra of FA-Au NCs are shown in figure 4. The FA-Au NCs spectrum contains FA-related peaks at 8.63, 7.68 and 6.84 ppm, confirming successful passivation of the Au NCs with folic acid functionalized capping ligands. The long-term stability of both targeted and non-targeted Au NCs was investigated with respect to optical and morphological properties. UV–vis spectroscopy, NMR and TEM studies were performed at different times over a period of at least 18 months and revealed no changes for the NCs properties (solutions were stored at 4 °C). The FA-Au NCs were found to be stable at pH values between 7 and 11, and at temperatures up to $T = 50$ °C. The long-term stability observed for our AuNCs and FA-Au NCs at physiologically relevant pH and temperature are promising for their further applications (see supplementary information S2).

To explore the effect of the Au NCs on cell viability, we selected three human-derived carcinoma cell lines: MCF-7 and MDA-MB-231 breast cancer cells, and HCT-116 colon cancer cells. Cell viability was assessed using the 3-(4,5-dimethylthizol-2-yl)-2,5-diphenyltetrazolium bromide (MTT) assay. Cells were seeded in 96 well plates and allowed 24 h to adhere, before exposure to Au NCs and FA-Au NCs ($\leqslant$0.5 mM; 72 h). No noticeable toxicity was observed over all the range of treatment concentrations (figures 5(a), (b) and supplementary information, S4). A small decrease in viable cell population of ~25% was observed for both agents at very high concentrations (0.1–0.5 mM).

In order to confirm FA targeting of Au NC, inductively coupled plasma mass spectrometry (ICP-MS) was used to estimate cellular uptake of NCs by the folic acid receptor expressing (FR+) human breast cancer cell line MDA-MB-231. The MDA-MB-231 cell line has the greatest abundance of folic acid receptors alpha (FRα), with 369 $\pm$ 6 fg/cell, (FAα, 38 kDa, 5.8 $\times$ 10^{6} $\pm$ 9.5 $\times$ 10^{4}/cell) while the MCF-7 cell line has 209 $\pm$ 5 fg/cell (3.3 $\times$ 10^{6} $\pm$ 7.9 $\times$ 10^{4}/cell) [28] and the HCT-116 expresses the lowest levels [16]. Cells were exposed to FA-Au NCs and Au NCs for 24 h prior to cell harvesting. The cellular uptake of both types of Au NCs by MDA-MB-231 cells is shown in figure 5(c) as weight ratio between the amount of gold uptaken and that used for cell treatment. Cell uptake assessment by ICP MS on FRα-negative A549, human lung cancer cell line, found comparable uptake of non-targeted and FA-functionalised Au NC, with only ~20% greater amount of Au detected in A549 cells exposed to FA-functionalised NCs. This increase is significantly lower compared to FR + MDA-MB-231 cells, where FA-targeted Au NCs are internalized by the cells in greater quantities (~2 fold enhancement) compared to non-targeted Au NCs (see supplementary information S4). Comparable increases in cell internalization of NP have previously been reported for FA-conjugated Fe_3O_4 [29].

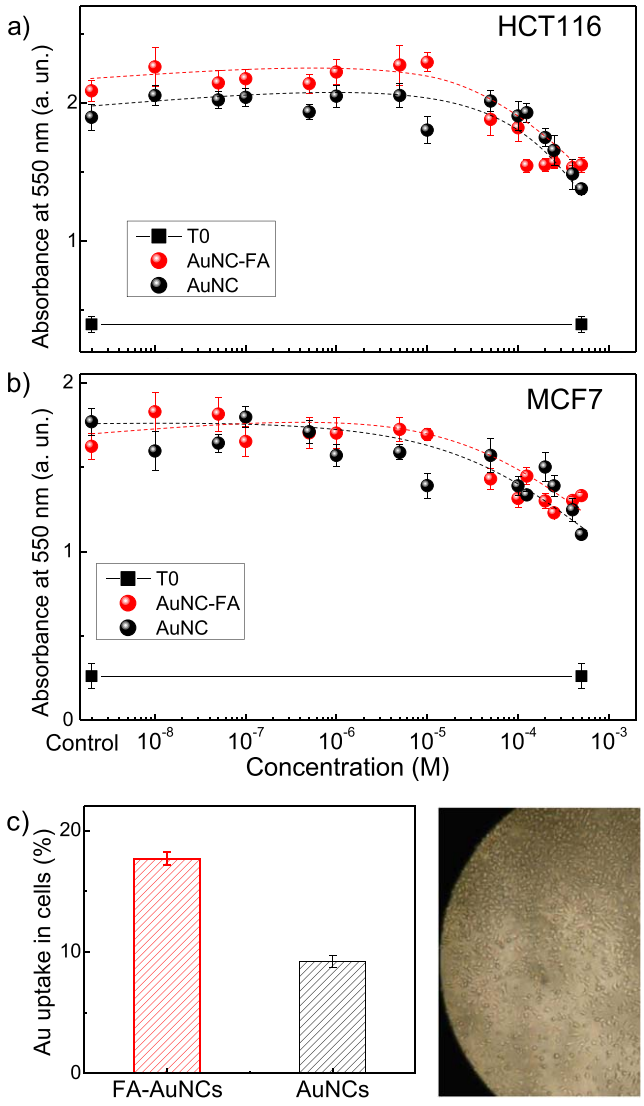

Figure 5. MTT assays results of PEG_{200}-AuNCs and FA-AuNCs on (a) MCF-7 and (b) HCT-116. Results are shown ±SD for $n = 9$. (c) Cellular uptake of FA-Au NCs and PEG-Au NC by FA over-expressing MDA-MB-231 cells following 24 h exposure. The uptake was quantified by ICP-MS.

In our conjugation method, there is no regioselectivity towards the α- or γ-carboxylic groups in the glutamic acid moiety of the FA. However, the chosen methodology enables readily accessible coupling that is known to produce up to 90% of γ-conjugates [30]. Further purification of γ-conjugates or direct synthesis of γ-conjugated FA-derivatives [31, 32] could offer improvements in targeting due to their higher affinity to folate receptors [31], and beneficial interactions of the free α-carboxylic group with residues within the receptor [33].

In conclusion, we have demonstrated successful synthesis of sub 2 nm diameter Au NCs and their successful passivation with FA-PEG-LA ligands. The FA-Au NCs are efficiently targeted to FA-overexpressing cancer cells, such as MDA-MB-231. Combined low cytotoxicity and enhanced cellular uptake are of interest for exploitation of these NCs in nanomedicine. Furthermore, the observed paramagnetism could herald exciting opportunities for targeted MRI. The imaging and therapy prospects of these NCs therefore merit future studies *in vivo*.

Experimental section

Experimental techniques

All reagents were obtained from Sigma-Aldrich Co. Ltd and were used without further purification. TLC analysis of reaction mixtures was performed using Merck Kieselgel 60 F_{254} plates; visualization was carried out by irradiation with a UV lamp (254 nm) and staining with phosphomolybdic acid or permanganate solution. ^{1}H and ^{13}C NMR spectra were recorded at ambient temperature with Bruker DPX 300, Bruker AV400, Bruker AV(III)400 or Bruker AV(III)500 spectrometers and were referenced to residual ^{1}H and ^{13}C signals of the deuterated solvents, respectively (δH 7.26, δC 77.00 for chloroform). The NMR spectra of NCs in water solution were collected at 600 MHz on a Bruker Avance III spectrometer at 298 K in H_2O:D_2O (1:9). For transmission electron microscopy (TEM) studies, the nanoparticles were deposited on a graphene oxide-coated grid and TEM images were recorded on a JEOL 2100 F FEGTEM microscope operating at 200 kV. The optical properties of Au NCs were measured in solution in quartz cuvettes with an Agilent Cary 100 UV–vis spectrometer at 25 °C. A commercial Quantum Design MPMS-XL5 SQUID magnetometer was used for the magnetic characterization of frozen solution samples frozen in quartz tubes with negligible diamagnetic contribution. Variable-temperature (1.8–20 K) and field-dependent (0–5 T) magnetization measurements were carried out using the reciprocating sample option with a sensitivity of 5×10^{-9} emu.

Synthesis of Au NCs with LA-PEG_{400}-R

For the synthesis of the capping ligands, the procedure from the [34] was adopted. LA-PEG_{400}-R (30 μmol) was dissolved in deionized water (20 ml) containing sodium hydroxide (50 μl, 2 M). Chloroauric acid (10 μl, 1 M in water, 0.01 mmol) was added and stirred gently for 5 min. Sodium borohydride (400 μl, 50 mM in water) was added dropwise and the resulting solution was moderately stirred overnight at room temperature. Crude Au NCs solution was centrifuged through AMICON column filters (10 kDa MW cut-off, 1 cycles @ 4000 g for 20 min), with the nanoparticles being collected over the membrane and dispersed in water. The resulting solution was stored at 4 °C.

Synthesis of FA-PEG-LA

For FA conjugation, 10 ml dimethyl sulfoxide (DMSO) was loaded in a 50 ml round bottom flask. FA (0.16 g, 0.36 mmol) was added into the flask and stirred until totally dissolved. *N*-(3-Dimethylaminopropyl)-*N*′-ethylcarbodiimide hydrochloride (0.104 g, 0.544 mmol) and *N*-hydroxysuccinimide (64 mg, 0.544 mmol) were added to the reaction and stirred

for 20 h in the dark. LA-PEG_{200}-NH_2 (0.4197 g, 1.08 mmol) was added to the mixture and further stirred for 16 h. The precipitate formed after the addition of acetone (50 mL) was collected and dissolved in 40 ml of ethyl acetate (EtOAc). The organic layer was washed with brine (50 ml, five times) and dried over anhydrous sodium sulphate (Na_2SO_4), concentrated under reduced pressure to yield the final product (HRMS expected value for $C_{35}H_{49}N_9O_9S_2$ $[M–H]^-$ is 802.3022 m/z, found 802.2991 m/z; see also supplementary information, S2).

Synthesis of Au NCs functionalized with FA

LA-PEG_{200}-FA (30 μmol) was dissolved in deionized water (20 ml) containing sodium hydroxide (50 μl, 2 M). Chloroauric acid (10 μl, 1 M, 0.01 mmol) was added and stirred gently for 5 min. Sodium borohydride solution (400 μl, 50 mM) was added dropwise and moderately stirred overnight at room temperate to obtain crude Au NCs. The solution obtained was purified by centrifugation (three times) using AMICON filters with a molecular weight cut-off of 10 kDa at 4000 g for 20 min per run. The resulting solutions were stored at $T = 4$ °C until further use.

In vitro characterization

For MTT assays, cells were seeded into a 96 well plate at a density of 3000 cells/well. Cells were allowed 24 h to adhere prior to treatment. Au NCs were tested at final concentrations between 10 nM and 0.5 mM. Following 72 h exposure of cells to Au NCs, 50 μl 2 mg ml^{-1} MTT was added. The plate was incubated for 2 h. Thereafter, medium and test agent were aspirated and formazan crystals dissolved in DMSO (150 μl per well). Absorbance values were read at 550 nm using an EnVision® Multilabel Plate Reader (PerkinElmer). Cell viability was estimated as percentage absorbance compared to untreated control cells.

Cellular uptake of Au NPs was assessed using ICP-MS. The cells were seeded into a six well plate at a density of 10^5 cells/well and incubated for 24 h. The medium was aspirated and treatment agent added (2 ml/well) at Au NC concentration of 10 μM. Following 24 h exposure, the medium was aspirated and the cells were washed with PBS (3 × 2 ml) to remove extracellular Au NCs. Then 16 M HNO_3 (14 ml) was added to digest cells for 30 min. The solution was diluted with deionized water to 5 ml for ICP-MS studies.

Acknowledgments

This work was supported by the National Centre for the Replacement, Refinement and Reduction of Animals in Research (Grant Number NC/L001861/1); the Engineering and Physical Sciences Research Council (Grant Numbers EP/K503800/1, NC/L001861/1); the China Scholarship Council, the Nanoscale and Microscale Research Centre and University of Nottingham. Authors are very grateful for assistance with ICP-MS and useful discussions with Dr Scott Young, and acknowledge useful discussions with Dr Graham Rance.

ORCID iDs

Lyudmila Turyanska https://orcid.org/0000-0002-9552-6501
Tracey D Bradshaw https://orcid.org/0000-001-8451-5092
Neil R Thomas https://orcid.org/0000-0002-9260-5423

References

[1] Shi J J, Kantoff P W, Wooster R and Farokhzad O C 2017 *Nat. Rev. Cancer* **17** 20
[2] Kinnear C, Moore T L, Rodriguez-Lorenzo L, Rothen-Rutishauser B and Petri-Fink A 2017 *Chem. Rev.* **117** 11476
[3] Jihye C, Kyung Oh J, Edward E G and Guillem P 2018 *Nanotechnology* **29** 504001
[4] Shang L, Dong S and Nienhaus G U 2011 *Nano Today* **6** 401
[5] Chen L-Y, Wang C-W, Yuan Z and Chang H-T 2015 *Anal. Chem.* **87** 216
[6] Jin R, Zeng C, Zhou M and Chen Y 2016 *Chem. Rev.* **116** 10346
[7] Zheng Y, Lai L, Liu W, Jiang H and Wang X 2017 *Adv. Colloid Interface Sci.* **242** 1
[8] Bagheri H, Afkhami A, Khoshsafar H, Hajian A and Shahriyari A 2017 *Biosens. Bioelectron.* **89** 829
[9] Yang X, Sun J-K, Kitta M, Pang H and Xu Q 2018 *Nat. Catal.* **1** 214
[10] Susumu K, Mei B C and Mattoussi H 2009 *Nat. Protoc.* **4** 424
[11] Jokerst J V, Lobovkina T, Zare R N and Gambhir S S 2011 *Nanomedicine* **6** 715
[12] Zebibula A, Alifu N, Xia L, Sun C, Yu X, Xue D, Liu L, Li G and Qian J 2017 *Adv. Funct. Mater.* **28** 1703451
Zamberlan F *et al* 2018 *J. Mater. Chem.* **6** 550–5
[13] Palui G, Aldeek F, Wang W and Mattoussi H 2015 *Chem. Soc. Rev.* **44** 193
[14] Suk J S, Xu Q, Kim N, Hanes J and Ensign L M 2016 *Adv. Drug Del. Rev.* **99** 28
[15] Qiao J, Mu X, Qi L, Deng J and Mao L 2013 *Chem. Commun.* **49** 8030
[16] Chen H, Li S, Li B, Ren X, Li S, Mahounga D M, Cui S, Gu Y and Achilefu S 2012 *Nanoscale* **4** 6050
Khlebtsov B, Tuchina E, Tuchin V and Khlebtsov N *RSC Adv.* 2015 **5** 61639
[17] Danhier F, Feron O and Préat V 2010 *J. Control. Release* **148** 135
[18] Keskin T, Yalcin S and Gunduz U 2018 *Inorg. Nano-Met. Chem.* **48** 150–9
[19] Chávez-García D, Juárez-Moreno K, Campos C H, Alderete J B and Hirata G A 2018 *J. Mater. Res.* **33** 191
[20] Zhang C, Zhang A, Hou W, Li T, Wang K, Zhang Q, de la Fuente J M, Jin W and Cui D 2018 *ACS Nano* **12** 4408
[21] Zhang Z W, Jia J, Lai Y Q, Ma Y Y, Weng J and Sun L P 2010 *Biorg. Med. Chem.* **18** 5528
[22] Zhang C *et al* 2015 *Adv. Funct. Mater.* **25** 1314
Zhang C, Zhou Z, Qian Q, Gao G, Li C, Feng L, Wang Q and Cui D 2013 *J. Mater. Chem.* B **1** 5045
Galchenko M, Schuster R, Black A, Riedner M and Klinke C 2019 *Nanoscale* **11** 1988
[23] Wang Y Q, Liang W S and Geng C Y 2009 *Nanoscale Res. Lett.* **4** 684

[24] Boles M A, Engel M and Talapin D V 2016 *Chem. Rev.* **116** 11220
[25] Trudel S 2011 *Gold Bull.* **44** 3
Nealon G L, Donnio B, Greget R, Kappler J-P, Terazzi E and Gallani J-L 2012 *Nanoscale* **4** 5244
[26] Moro F, Turyanska L, Wliman J, Williams H E L, Fielding A and Patanè A 2016 *Nano Lett.* **16** 6343
[27] Matias R, Ribeiro P R S, Sarraguça M C and Lopes J A 2014 *Anal. Methods* **6** 3065
[28] Yang T, Xu F, Fang D and Chen Y 2015 *Sci. Rep.* **5** 16733
[29] Rana S, Shetake N G, Barick K C, Pandey B N, Salunke H G and Hassan P A 2016 *Dalton Trans.* **45** 17401
[30] Kim D *et al* 2007 *Angew. Chem. Int. Ed.* **46** 3471
[31] Wang S, Luo J, Lantrip D A, Waters D J, Mathias C J, Green M A and Fuchs P L 1997 *Bioconjugate Chem.* **8** 673
[32] Trindade A F, Frade A, Maçôas E M, Graça C, Rodrigues C A, Martinho J M and Afonso C A 2014 *Org. Biomol. Chem.* **12** 3181
[33] Chen C, Ke J, Zhou X E, Yi W, Brunzelle J S, Li J, Yong E-L, Xu H E and Melcher K 2013 *Nature* **500** 486
[34] Mei B C, Susumu K, Meidintz I L and Mattoussi H 2009 *Nat. Protocols* **4** 412